STORE OPERATED CALCIUM ENTRY SUPPRESSED TGFβ1-SMAD3 SIGNALING PATHWAY IN GLOMERULAR MESANGIAL CELLS

Sarika Chaudhari[1], Weizu Li[1, 2], Yanxia Wang[1], Hui Jiang[1, 3], Yuhong Ma[1, 4], Mark E. Davis[5], Jonathan E. Zuckerman[5], and Rong Ma[1*]

1: Institute for Cardiovascular and Metabolic Diseases, University of North Texas Health Science Center, Fort Worth, Texas 76107

2: Department of Pharmacology, Anhui Medical University, Hefei, China 230032

3: The first hospital affiliated to Anhui University of Traditional Chinese Medicine, Hefei, China 230032

4: Department of Clinical Medicine, Wanna Medical College, Wuhu, Anhui, China 241002

5: Chemical Engineering, California Institute of Technology, Pasadena, CA 91125

Running Title: Suppression of TGFβ1/Smad3 pathway by SOCE

*: To whom correspondence should be addressed:

3500 Camp Bowie Blvd.

Department of Integrative Physiology and Anatomy

University of North Texas Health Science Center

Fort Worth, TX 76107

Tel: 817-735-2516; Fax: 817-735-5084

E-mail: rong.ma@unthsc.edu

ABSTRACT

Our previous study demonstrated that the abundance of extracellular matrix proteins was suppressed by store-operated Ca^{2+} entry in mesangial cells (MCs). The present study was conducted to investigate the underlying mechanism focused on the transforming growth factor beta 1 (TGFβ1) - Smad3 pathway, a critical pathway for ECM expansion in diabetic kidneys. We hypothesized that SOCE suppressed ECM protein expression by inhibiting this pathway in MCs. In cultured human MCs, we observed that TGFβ1 (5 ng/ml for 15 hours) significantly increased Smad3 phosphorylation as evaluated by immunoblot. However, this response was markedly inhibited by thapsigargin (1 μM), a classical activator of store-operated Ca^{2+} channel. Consistently, both immunocytochemistry and immunoblot showed that TGFβ1 significantly increased nuclear translocation of Smad3 which was prevented by pre-treatment with thapsigargin. Importantly, the thapsigargin effect was reversed by Lanthanum (La^{3+}) (5 μM) and GSK-7975A (10 μM), both of which are selective blockers of store-operated Ca^{2+} channel. Furthermore, knockdown of Orai1, the pore-forming subunit of store-operated Ca^{2+} channel, significantly augmented TGFβ1-induced Smad3 phosphorylation. Overexpression of Orai1 augmented the inhibitory effect of thapsigargin on TGFβ1-induced phosphorylation of Smad3. In agreement with the data from cultured MCs, *in vivo* knockdown of Orai1 specific to MCs using a targeted nanoparticle siRNA delivery system resulted in marked increase in abundance of phosphorylated Smad3 and in nuclear translocation of Smad3 in glomerulus of mice. Taken together, our results indicate that store-operated Ca^{2+} entry in MCs negatively regulates the TGFβ1-Smad3 signaling pathway.

KEYWORDS

mesangial cells, store-operated Ca^{2+} entry, Orai1, TGFβ1, Smad3

INTRODUCTION

Progressive accumulation of extracellular matrix (ECM) proteins in the glomerulus is one of the consistent pathological changes initiated at an early stage in kidney diseases such as diabetic nephropathy (DN) (24; 47). The magnitude of matrix accumulation in both the glomeruli and the interstitium is intensely and independently associated with the degree of renal insufficiency and proteinuria in patients with the renal dysfunction (51). Over extended period of time, the ECM accumulation and its dysregulated remodeling contributes to irreversible fibrotic changes that lead to chronic kidney disease and ultimately kidney failure in the form of end stage renal disease (13; 45). Glomerular mesangial cells (MCs) which are one of the major sources of ECM proteins are also an important target of metabolic abnormalities in diabetic environment (1; 18). Since ECM expansion in the mesangium is one early feature of DN (47), it is important to study the mechanisms that regulate ECM dynamics in MCs.

Store operated Ca^{2+} entry (SOCE), which regulates many physiological and pathological functions in variety of cells, is an important Ca^{2+} signaling pathway in MCs (29; 35; 43). In our previous study, we demonstrated a negative effect of SOCE on the content of ECM proteins like fibronectin and collagen-IV (Col IV) in MCs (61), suggesting an anti-fibrotic effect of SOCE in MCs. However, the mechanism underlying the inhibitory effect of SOCE on ECM protein expression is not known. Transforming growth factor beta1 (TGFβ1), a multifunctional cytokine, plays a critical role in ECM protein dynamics (17; 19; 37; 40). It exerts its potent fibrotic effect intracellularly via receptor operated Smad (R-Smad) proteins, particularly Smad3 (21; 26; 44; 46; 55; 56). Activation of Smad3 by TGFβ1 through phosphorylation and subsequent translocation into the nucleus, regulates the transcription of target genes including those encoding or regulating ECM proteins (4; 12; 25; 26). In this study, we investigated if SOCE-induced suppression of fibronectin and Col IV was mediated by inhibition of the TGFβ1-Smad3 pathway.

91

MATERIAL AND METHODS

Mesangial Cell culture Human MCs were purchased from Lonza (Catalogue no:CC2559, Walkersville, MD). MCs in a 75-cm^2 flask were cultured in 5.6 mM glucose DMEM (GIBCO, Carlsbad, CA) supplemented with 25 mM HEPES, 4 mM glutamine, 1.0 mM sodium pyruvate, 0.1 mM nonessential amino acids, 100 U/ml penicillin, 100 μg/ml streptomycin, and 20% fetal bovine serum (FBS). When MCs reached 90% confluence, the cells were split into 60 mm or 35 mm culture plates for various treatments as specified in figure legends. The cell growth was arrested with 0.5% FBS medium during treatments. The culture media was replaced every 2 days with fresh media. Activators or inhibitors of SOCE were added 20 min before TGFβ1 treatment. Cells used were with sub-passages not more than nine generations.

Transient transfection of human MCs Small interfering (si) RNA against human Orai1 or scrambled control siRNA (both 50 nM) were transfected into human MCs using Dharmafect 2 transfection reagent (Thermo Scientific, Rockford, IL) in serum free DMEM media following the protocol provided by the manufacturer. Media was changed to 20% FBS DMEM media after 6 h. Cells were harvested for Western blot 72 h after transfection. Expression plasmid of Orai1 (FLAG-Orai1) and empty vector (yellow fluorescent protein, YFP) were transfected into MCs at 0.5 μg/ml using Lipofectamine and Plus reagent (Invitrogen-BRL, Carlsbad, CA) following the protocols provided by the manufacturer. Cells were collected 48 h after transfection for immunoblot analysis.

Preparation of nuclear extracts Preparation of nuclear extracts from human MCs was performed using NE-PER Nuclear and Cytoplasmic Extraction Reagents (Catalogue No: 78833, Thermo Scientific, Rockford, IL) following the manufacturer's protocol. The extracts were stored at -80^0C until use.

Immunoblot Analysis Immunoblot analysis was performed as described in our previous publications (7). Briefly, the whole-cell lysates were fractionated by 10% SDS-PAGE, transferred to

PVDF membranes, and probed with primary antibodies to Smad3, phospho-Smad3 (p-Smad3), Orai1, TGFβ1, FLAG, TATA binding protein (TBP) and tubulin. Bound antibodies were visualized with Super Signal West Femto or Pico Luminol/ Enhancer Solution (Catalogue No: 34095 and 34087, Thermo Scientific, Rockford, IL). The specific protein bands were visualized and captured using the AlphaEase FC Imaging System (Alpha Innotech, San Leandro, CA). The integrated density value (IDV) of each band was measured by drawing a rectangle outlining the band using AlphaEase FC software with autobackground subtraction. In term of p-Smad3 (Figs. 2-5), we only measured the IDV of the major band at a molecular size of ~60 kDa, which represents p-Smad3 protein. The expression of TGFβ1 protein was quantified by normalization of the IDV of the protein band to that of tubulin band on the same blot. The expression of p-Smad3 protein was quantified by normalization of the IDV of p-Smad3 bands to that of Smad3 band on the same blot except Fig. 5 in which the expression of nuclear p-Smad3 protein was normalized to TBP.

ELISA Abundance of TGFβ1 in supernatant media was determined by a solid-phase sandwich enzyme-linked immunosorbent assay (ELISA) using a DuoSet ELISA Development kit for TGFβ1 (Catalogue No: DY240-05**,** R&D System, Minneapolis, MN, USA). Briefly, MCs were plated in 24 well plates as 1.8×10^4 cells per well. When cells were confluent, they were serum deprived till the end of experiment. SOCE was activated by treating these cells with 1μM thapsigargin (TG) for 8 h before collection of their supernatant. The collected supernatant media was centrifuged at 1500 rpm for 10 min at 4^0C and stored at -80^0C until use. Latent TGFβ1 in the cell supernatants was activated with acidification of samples by 1.0 N HCl and subsequent neutralization with 1.2 N NaOH/0.5 M HEPES and assayed immediately using the protocol provided by the manufacturer. The optical density was determined using the microplate reader set to 450 nm. TGFβ1 concentration in the media was determined from the standard curve obtained using the Sigma plot software version 11.

Immunofluorescence Cytochemistry Human MCs were plated on 22 × 22 × 1 mm glass coverslips in 35-mm culture dishes. Cells were treated with TGFβ1 (5 ng/ml) for 15 h, with or without TG (1μM) and GSK-7975A (10 μM). GSK-7975A was added 20 min before addition of TG which was applied 20 min prior to TGFβ1 treatment. After 15 h, cells were washed with PBS and fixed with 4% paraformaldehyde for 15 min at room temperature. After another wash with PBS, the cells were then incubated with ice-cold acetone at -20°C for 10 min. After 30 min of incubation with blocking buffer, the cells were incubated with mouse anti-Smad3 primary antibody at 1:100 in PBS plus 10% donkey serum and 0.2% Triton X-100 at 4 °C overnight. After three washes with PBS, the cells were then incubated with donkey anti-mouse secondary antibody conjugated with Alexa Fluor 568 (Catalogue No: A10037, Invitrogen) at a concentration of 1:500 for 1 h at 4^0C in dark. 4', 6-diamidino-2-phenylindole (DAPI, Catalogue No: H-1200, Invitrogen) was used for staining nuclei. Fluorescent staining was examined using an Olympus microscope (BX41) equipped for epifluorescence and an Olympus DP70 digital camera with DP manager software (version 2.2.1). Images were converted to 16-bit format and uniformly adjusted for brightness and contrast using ImageJ (version 1.47; NIH).

Fluorescence Measurement of $[Ca^{2+}]_i$ Measurements of $[Ca^{2+}]_i$ in human MCs using fura-2 were performed using dual excitation wavelength fluorescence microscopy. MCs grown on a coverslip (22 × 22 mm) were loaded with 2 μM acetoxymethyl ester of fura-2 (fura-2/AM) plus 0.018 g/dl Pluronic F-127 (Invitrogen, Grand Island, NY) for 50 min at room temperature followed by additional 20 min incubation in fura-2 free physiological saline solution. The coverslip was then placed in a perfusion chamber (Warner, Model RC-2OH) mounted on the stage of a Nikon Diaphot inverted microscope. Fura-2 fluorescence was monitored at 340 and 380 nm excitation wavelengths and at 510 nm emission wavelength using NIS Elements AR^{TM} software (Nikon Instruments Inc., Melville, NY) at room temperature. $[Ca^{2+}]_i$ was calculated using the software following the manufacturer's instructions. Calibrations were performed at the end of each experiment, and conditions of high $[Ca^{2+}]_i$ were achieved

by addition of 5 μM ionomycin, whereas conditions of low $[Ca^{2+}]_i$ were obtained by addition of 5 mM EGTA.

Animals All procedures were approved by the University of North Texas Health Science Center (UNTHSC) Institutional Animal Care and Use Committee. Ten male C57BL/6 mice were purchased from Charles River Laboratories (Wilmington, MA). All mice used in this study were between 2 and 4 months of age. The animals were maintained at the animal facility of UNTHSC under local and National Institutes of Health guidelines.

***In Vivo* Delivery of nanoparticles (NPs) into the Kidney of Mice** The targeted NP-delivery system was used to deliver siRNA against Orai1 to the kidney of mice as previously described (61; 65). The compositions and formulation of the NP/siRNA complex were described previously (65). Mice were randomly divided into control and Orai1–knocked down groups (five mice in each group). Tail vein injection of NPs containing Cy3- tagged siRNA against mouse Orai1 (NP-Cy3- siOrai1) were given at a dose of 10 mg/kg siRNA in a volume of 100 μl to the mice in the Orai1–knocked down group. The mice in the control group were only given unconjugated NPs through the same route at the same injection volume. These intravenous injections were given on day 1 and 3 of the experiment and the mice were euthanized on day 5. Mice were euthanized via intraperitoneal injection of pentobarbital (100 mg/kg body weight). Kidneys were perfused with PBS to wash out the blood and the left kidney was removed and fixed in 4% paraformaldehyde. Paraformaldehyde-fixed kidney was embedded in molten paraffin and then, was sectioned at 4 μm in thickness (Cryostat 2800 Frigocut-E; Leica Instruments) for immunohistochemical examination.

Immunofluorescent staining Anti α8 integrin rabbit polyclonal antibody at 1:50 and Alexa Fluor 488 Donkey anti-rabbit IgG (Catalogue no: A21206, Invitrogen, Eugene, OR) at 1:200 were used to label mouse glomerular MCs. Anti-synaptopodin goat polyclonal antibody at 1:50 and Alexa Fluor 488 donkey anti goat IgG (Catalogue no: A11055, Life Technologies, Eugene, OR) at 1:200 was used to

label the podocytes. Sections were visualized using an Olympus microscope (BX41) equipped for epifluorescence and an Olympus DP70 digital camera with DP manager software (version 2.2.1). Images were converted to 16-bit format and uniformly adjusted for brightness and contrast using Image J (version 1.50b, NIH).

Immunohistochemistry After rehydration, antigen retrieval was achieved by heating the sections in 10 mM citrate buffer in a microwave for 10 min. The sections were blocked by 5% goat serum for 30 min at room temperature and then were incubated with anti p-Smad3 rabbit antibody at 1:100 at 4^0C overnight. The sections were incubated with anti-rabbit poly HRP IHC reagent (Catalogue no: IHC-2291, General Bioscience Corporation) at room temperature for 1 h, followed by incubation with peroxidase substrate solution for about 2-3 min, dipping the slides in hematoxylin solution for 90 seconds, dehydration in incubator at 60^0C for 30 min and cover slips with mounting media containing DAPI. Sections were examined using an Olympus microscope (BX41) and an Olympus DP70 digital camera with DP manager software (version 2.2.1). Images were uniformly adjusted for brightness and contrast and converted to 8-bit format for measuring intensity of staining using Image J (version 1.50b, NIH).

Materials Primary antibodies against p-Smad3 (ab51451) and TBP (ab818) were purchased from Abcam (Cambridge, MA). Primary antibodies against Smad3 (sc101154), integrin α8:H-180 (sc-25713), synaptopodin (P-19) (sc-21537) and α-tubulin (sc-5286) were purchased from Santa Cruz Biotechnologies (Dallas, TX). Primary antibodies against Orai1 (O8264) and FLAG fusion proteins (A8592) were purchased from Sigma-Aldrich, (Israel). Secondary antibodies for western blot, goat anti mouse Ig HRP (sc2005) and goat anti rabbit Ig HRP (sc2003) were purchased from Santa Cruz Biotechnologies. Small interfering (si) RNA against human Orai1and Cy3–labeled siRNA against mouse Orai1 were purchased from Integrated DNA Technologies, Inc. (Chicago, IL) (Table 1). Scramble control siRNA (ON-TARGETplus Non-targeting control siRNA#1) (D-001810-01-20) was

purchased from Dharmacon, GE. mCherry- Red-Orai1/p3X FLAG-CMV 7.1 expression plasmid was obtained from Dr. Yuan at UNTHSC.

TG (T9033) and Hematoxylin (GHS3) were purchased from Sigma-Aldrich. Human recombinant TGFβ1 (240-B-002) was purchased from R&D systems. GSK-7975A was kindly donated by GlaxoSmithKline (Brentford, UK). Peroxidase substrate solution (DAB Peroxidase substrate kit SK-4100) was purchased from Vector Laboratories (Burlingame, CA).

Statistical Analyses Data were reported as mean ± SEM. The one-way repeated measures of ANOVA plus Student-Newman–Keuls post hoc analysis and unpaired t-test were used to analyze the differences among multiple groups and between two groups, respectively, unless indicated in individual figures. $P<0.05$ was considered statistically significant. Statistical analysis was performed using SigmaStat (Jandel Scientific, San Rafael, CA).

RESULTS

SOCE activation did not alter amount of secreted TGFβ1 by human MCs.

MCs are known to synthesize and secrete TGFβ1 (23; 58; 62). To study if Ca^{2+} entry via store-operated Ca^{2+} channel, i.e. SOCE affected secretion of TGFβ1 by MCs, we activated store-operated Ca^{2+} channel by treating the cells with 1 μM TG for 8 and 15 h. ELISA assay showed that TG treatment for both time periods did not significantly change the concentration of TGFβ1 in the cell culture media (Fig. 1). These results indicate that SOCE did not affect the amount of secreted TGFβ1 protein by MCs.

SOCE inhibited TGFβ1 induced phosphorylation of Smad3.

A variety of stimuli such as Angiotensin II, high glucose, advanced glycosylation end products, and reactive oxygen species activate TGFβ1 to regulate expression of matrix proteins by MCs (16; 22; 53). One of the major intracellular downstream pathways mediating this effect has been demonstrated to be via the activation of Smad proteins, particularly Smad3 (14; 25; 27; 30; 31; 48). In agreement with those studies, we also found that administration of TGFβ1 (5 ng/ml), but not its vehicle control (HCl) for 15 h induced a robust increase in the content of phospho-Smad3, the active form of Smad3, in human MCs (Fig. 2 A&B). Activation of store-operated Ca^{2+} channel by TG significantly attenuated the TGFβ1 response. However, the content of total Smad3 did not have significant change. These results indicate that SOCE inhibits activation of the TGFβ1-Smad3 pathway in MCs.

Knockdown of Orai1 increased while overexpression of Orai1 decreased the TGFβ1-induced phosphorylation of Smad3.

Further, we speculated that knocking down the pore forming unit of store-operated Ca^{2+} channel may have an opposite effect to that of activation of the channel. Indeed, TGFβ1-induced phosphorylation of Smad3 was further and significantly increased in human MCs transfected with Orai1 siRNA as compared to untransfected cells and scramble siRNA-transfected cells. (Fig3 A&B). Simultaneous activation of store-operated channel using 1 μM TG attenuated the enhanced response.

Western blot showed that Orai1 protein abundance was significantly reduced by its siRNA treatment (Fig. 3A).

To support these findings, we next overexpressed Orai1 protein in human MCs with FLAG-Orai1. The expressed Orai1 band was detected at approximately 80 kDa (Fig. 4C). As shown in Fig. 4 A&B, activation of SOCE by TG significantly decreased TGFβ1-induced phosphorylation of Smad3. This inhibition was further augmented by overexpressing Orai1. To verify if the expressed Orai1 was functional, we carried out Ca^{2+} imaging experiments to measure SOCE in human MCs with and without expressing Orai1 using a classical Ca^{2+} re-addition protocol (35). As shown in Fig. 4D, the TG-stimulated SOCE response was significantly greater in human MCs transfected with FLAG-Orai1 compared with the response in MCs without transfection or transfected with YFP control plasmid.

SOCE decreased TGFβ1-mediated nuclear translocation of Smad3 in human MCs.

Activation of Smad3 by TGFβ1 involves its phosphorylation and subsequent translocation to the nucleus where it regulates the transcription of target genes. Published study demonstrated that TGFβ1 at 5 ng/ml stimulated nuclear translocation of Smads 15 h after treatment (57). We thus examined abundance of phosphorylated Smad3 in the nuclear extracts of human MCs treated with TGFβ1 at 5 ng/ml for 15 h with or without activation of store-operated Ca^{2+} channel. As shown in Fig. 5 A&B, translocation of phosphorylated Smad3 to the nucleus was significantly increased by TGFβ1 treatment. TG significantly reduced this translocation while simultaneous treatment with La^{3+} at 5 μM, which we have previously shown to block store-operated Ca^{2+} channel in human MCs (35), reversed the TG effect. Consistently, immunofluorescence study showed that Smad3 was localized in the cytosol in a large population of human MCs without stimulation. However, in the cells treated with TGFβ1, Smad3 was predominantly localized in the nucleus. TG inhibited this translocation, indicated by presence of Smad3 in the cytosol. The inhibitory effect of TG was abolished when the cells were simultaneously treated with a selective inhibitor of store-operated Ca^{2+} channel, GSK-7975A (10 μM) (Fig. 5 C&D).

***In Vivo* knockdown of Orai1 in MCs increased phosphorylation and nuclear translocation of Smad3 in mice.**

We next verified our *in vitro* findings in mice with knockdown of Orai1 in MCs using the established targeted NP-siRNA delivery system (64; 65). In our previous study, we injected the NP carriers containing Cy3-tagged siRNA against mouse Orai1 (NP-Cy3-siOrai1) into mice via the tail vein twice one week (61). We showed that the abundance of Orai1 protein was significantly reduced in the renal cortex from the mice receiving NP-Cy3-siOrai1 (61). During the one week of treatment period, there was no change in body weight, food intake and 24 h urine output in the mice treated with NP-Cy3-siOrai1 (data not shown). Using the kidney sample from that study, we conducted a series of immunofluorescence examinations. Consistent with our previous studies (61; 65), these NP-siRNA complexes were predominantly distributed in glomeruli with limited distribution in surrounding tubules (Fig. 6A). Next, we counterstained kidney sections from mice that received NP-Cy3-siOrai1 with a MC marker integrin α8 and a podocyte marker synaptopodin. As shown in Fig. 6B, the NP-Cy3-siOrai1 complexes highly co-localized with the integrin α-8, but were not colocalized with synaptopodin, suggesting that the NP-siRNA complexes were selectively delivered into MCs.

We next conducted immunohistochemical examination of the kidney sections from the mice with and without knockdown of Orai1. Smad3 protein was probed with the primary antibody of anti-phospho-Smad3, shown as brown color. The cell nucleus was stained with DAPI, shown as purple color. We found that in the mice treated with NP alone, the staining of phosphorylated Smad3 was mild. It was also observed that some glomerular cells did not have nuclear localization of Smad3, indicated by separate purple spots (Fig. 7 A&B). However, in the mice receiving NP-Cy3-siOrai1 the Smad3 staining in the glomeruli was markedly increased. Also, there were fewer cells without nuclear distribution of Smad3 (Fig. 7 A&B). Summary data showed a significant increase in the total intensity of Smad3 staining and a significant decrease in the number of cells without nuclear localization of Smad3 in the

mice treated with Orai1 siRNA (Fig. 7 C&D). Because the Orai1 siRNAs were specifically delivered to MCs (Fig. 6), these data suggest that knocking down Orai1 in MCs increased abundance of Smad3 and promoted nuclear translocation of Smad3.

DISCUSSION

SOCE is a ubiquitous intracellular Ca^{2+} signaling pathway, serving diverse functions in many non-excitable and excitable cells (15; 28; 35; 42; 52; 54). Apart from its physiological functions, this pathway is also involved in many pathological disorders. For instance, an altered SOCE is associated with many diabetic complications (6). We have previously demonstrated that SOCE in MCs suppressed ECM protein expression (61). It is known that multiple pathways regulate synthesis and degradation of ECM proteins and thus, affect expression level of ECM proteins (11; 34). TGFβ1, a pleotropic cytokine and the most common and best characterized isoform of TGFβ, is a known pro-fibrotic factor to stimulate production of ECM proteins in MCs (48). Also, TGFβ1 signaling pathway plays a critical role in mesangial expansion and renal fibrosis in diabetic kidney disease (17; 19). Serum levels of TGFβ1 are positively correlated with the severity of diabetic nephropathy (DN), while in diabetic patients without DN those are not significantly different as compared to nondiabetic subjects (40). Various studies have indicated that the potent fibrotic effect of TGFβ1 to be mediated via the receptor operated intracellular Smad signaling, particularly through Smad3 (14; 21; 26; 27; 46). Our results from the present study suggest that TGFβ1/Smad3 pathway is a target of SOCE for inhibition of ECM protein expression.

SOCE could inhibit the TGFβ1-Smad3 signaling by acting on one or more sites of this pathway in MCs. First, it could inhibit the production or secretion of TGFβ1 by MCs. Second, SOCE could inhibit the activation of Smad3, i.e. its phosphorylation, and the third, SOCE could inhibit the nuclear translocation of Smad3. Our findings suggest that SOCE may not influence TGFβ1 production and secretion by MCs in presence of NG because activation of SOC did not change the abundance of TGFβ1 in MCs and in media culturing MCs (Fig. 1).

Further our study suggests that activation (phosphorylation) and nuclear translocation of Smad3 are the regulatory sites for SOCE-induced inhibition of TGFβ1/Smad3 pathway. Receptor activation after TGFβ1 binding, leading to C-terminal phosphorylation of R-Smad is an important step which

destabilizes Smad interaction with Smad anchor for receptor activation (SARA), allowing dissociation of Smad from the complex and the subsequent exposure of a nuclear import region on the Smad MH2 domain (63). In addition, R-Smad phosphorylation augments its affinity for Smad4 (49). The association of these two proteins translocates to the nucleus and interacts with transcriptional regulation complexes. In this study, activation of SOC significantly reduced the TGFβ1-induced phosphorylation of Smad3 in MCs (Fig. 2). However, the abundance of total Smad3 remained unaffected. Since phosphorylated Smad3 is the active form of Smad3, a decrease in the ratio of p-Smad3 to total Smad3 indicates an inhibition of the Smad3 signaling pathway.

The inhibitory effect of SOCE on Smad3 activation (phosphorylation) was further supported by the data from experiments of manipulating Orai1 protein expression. Orai1 is the pore forming unit of store-operated Ca^{2+} channel and therefore, knocking down this channel protein would be expected to reduce SOCE. Consistent with the findings described above, knocking down Orai1 significantly enhanced TGFβ1-induced phosphorylation of Smad3 in human MCs (Fig. 3 A&B). In agreement with the results, over expressing Orai1 significantly augmented the inhibitory effect of SOCE on TGFβ1-stimulated Smad3 phosphorylation (Fig. 4). These findings are also in line with our previous reports that Orai1 knocked down increased ECM protein expression in MCs (61). Interestingly, one group recently reported that phosphorylation of Smad2/Smad3 was decreased by knocking down Orai1 in HK2 cells (36). However, if this decrease was specifically due to decrease in both Smad2 and Smad3 or only Smad2 or Smad3 was not clear. This is important because Smad2 and Smad3 may have totally opposite downstream effects, Smad3 being pro-fibrotic and Smad2 as anti-fibrotic, as demonstrated by many studies (10; 38). Another possibility is that the effect of SOCE is cell type or cell context specific. Also, some studies have reported that SOCE was decreased by overexpressing Orai1 alone (20; 39; 50) However, it might not be the case in human MCs. It might be that human MCs have spare STIM1

proteins and hence, overexpression of Orai1 may not change the stoichiometry of Orai1/STIM1 complexes

It is not known how SOCE inhibited phosphorylation of Smad3 by TGFβ1 from this study. Several possibilities exist. At the level of TGFβ receptor, SOCE may inhibit the type II or type I receptor kinase which in turn, suppresses the subsequent phosphorylation of Smad3. Another mechanism could be that SOCE either activates a Ca^{2+} dependent phosphatase, such as calcineurin or a receptor specific phosphatase PP1c that dephosphorylate TGFβ receptor I (5) reducing the subsequent Smad3 phosphorylation and thus inhibiting its activation and translocation. Alternatively, SOCE could facilitate the interaction between inhibitory Smad7 and the TGFβ receptors, resulting in suppression of downstream TGFβ1/R-Smad signaling, including phosphorylation of R-Smad.

Phosphorylation of Smad3 renders the receptor-operated Smad protein suitable for nuclear import, a critical step for its regulation of gene transcription. Because SOCE inhibited Smad3 phosphorylation, it is not surprising that the nuclear translocation of Smad3 was depressed by activation of store-operated channel and was promoted by inhibition of the channel (Fig. 5). However, the content of nuclear Smad3 is regulated by multiple mechanisms. The change in nuclear Smad3 in response to SOCE may not only be secondary to its inhibition on phosphorylation. Effect of SOCE on other pathways regulating nuclear localization of Smad3 can't be ruled out. For example, SOCE may also facilitate phosphorylation in the linker region by cyclin dependent kinases (CDKs) or mitogen associated protein kinases (MAPKs) rendering Smad3 unsuitable for nuclear transport or interacts with other kinases that can affect interaction of Smad3 with import machinery like nucleoporins, nuclear retention factors (8; 33; 59). Increased export of Smad3 out of the nucleus can also be a mechanism for suppressed nuclear content of phosphorylatedSmad3 by SOCE. Nuclear localized protein phosphatase PP1MA/PP2Cα, a Smad2/3 SXS-motif specific phosphatase, dephosphorylates Smad2/3 in the nuclei

and also facilitates the interaction of dephosphorylated Smad2/3 with a nuclear export factor, RanBP3 (Ran-binding protein 3) (32).

TGF-β/bone morphogenetic protein-Smad signaling involves multiple types of R-Smads that may have distinct target proteins. Classically, Smad2/3 stimulates production of fibronectin and connective tissue growth factor (12; 25; 26) while Smad1 promotes collagen IV production (3). These Smad signaling pathways are present in MCs (2; 3; 9; 41; 46; 60). We have demonstrated that SOCE inhibited production of both fibronectin and collagen IV proteins by MCs (61). In a recent study, we found that the inhibitory effect of SOCE on collagen IV protein production was through suppression of Smad1 pathway (60). In the present study, we showed that SOCE inhibited Smad3 signaling. Because Smad3 is the classic downstream pathway mediating TGF-β1-stimulated fibronectin production (12; 25; 26), the negative regulation of Smad3 signaling possible is the mechanism underlying SOCE-induced downregulation of fibronectin. Therefore, SOCE in MCs may regulate different ECM proteins through distinct Smad pathways, Smad1 for collagen IV and Smad3 for fibronectin.

In summary, we defined a negative regulation of TGFβ1-Smad3 pathway by SOCE in MCs. This inhibition was through suppression of phosphorylation and nuclear translocation of Smad3, but not by decreasing abundance of TGFβ1 protein in MCs. This mechanism is illustrated in Fig. 8. Because the Smad signaling pathway plays a crucial role in matrix protein production and renal fibrosis in many kidney diseases, our findings highlight that store-operated Ca^{2+} channel may be considered as an alternative therapeutic option for treating patients with renal fibrosis.

ACKNOWLEDGMENTS

We thank GlaxoSmithKline (Brentford, UK) for providing GSK-7975A compound and Dr. Joseph Yuan at University of North Texas Health Science Center at Fort Worth for providing the expression plasmid for human Orai1 (mCherry- Red-Orai1/p3X FLAG-CMV 7.1).

GRANTS

The work was supported by National Institutes of Health Grant RO1-DK079968 from the National Institute of Diabetes and Digestive and Kidney Disease (Ma), American Heart Association Southwest Affiliate Grant-in-Aid (16GRNT27780043, Ma), an Award from the Harry S. Moss Heart Trust (Ma), and Grant-in-Aid Research Grant for doctoral student from Sigma Xi (Chaudhari).

DISCLOSURE

All authors declared no competing interests.

REFERENCES

1. **Abboud HE**. Mesangial cell biology. *Exp Cell Res* 318: 979-985, 2012.
2. **Abdel-Wahab N, Wicks SJ, Mason RM and Chantry A**. Decorin suppresses transforming growth factor-b-induced expression of plasminogen activator inhibitor-1 in human mesangial cells through a mechanism that involves Ca^{2+}-dependent phosphorylation of Smad2 at serine-240. *Biochem J* 362: 643-649, 2002.
3. **Abe H, Matsubara T, Iehara N, Nagai K, Takahashi T, Arai H, Kita T and Doi T**. Type IV collagen is transcriptionally regulated by Smad1 under advanced glycation end product (AGE) stimulation. *J Biol Chem* 279: 14201-14206, 2004.
4. **Attisano L and Wrana JL**. Smads as trnascriptional co-modulators. *Curr Opin Cell Biol* 12: 235-243, 2000.
5. **Bennett D and Alphey L**. PP1 binds Sara and negatively regulates Dpp signaling in Drosophila melanogaster. *Nat Genet* 31: 419-423, 2002.
6. **Chaudhari S and Ma R**. Store-operated calcium entry and diabetic complications. *Exp Biol Med* 241: 343-352, 2016.
7. **Chaudhari S, Wu P, Wang Y, Ding Y, Yuan J, Begg M and Ma R**. High glucose and diabetes enhanced store-operated Ca^{2+} entry and increased expression of its signaling proteins in mesangial cells. *Am J Physiol Renal Physiol* 306: F1069-F1080, 2014.
8. **Chen X and Xu L**. Mechanism and regulation of nucleocytoplasmic trafficking of Smad. *Cell Bioscien* 1: 40, 2011.
9. **Chen Y, Blom IE, Sa S, Goldschmeding R, Abraham DJ and Leask A**. CTGF expression in mesangial cells: involvement of SMADs, MAP kinase, and PKC. *Kidney Int* 62: 1149-1159, 2002.
10. **Duan W, Yu X, Huang X, Yu J and Lan HY**. Opposing roles for Smad2 and Smad3 in peritoneal fibrosis in vivo and in vitro. *Am J Pathol* 184: 2275-2284, 2014.
11. **Eddy AA**. Molecular basis of renal fibrosis. *Pediatr Nephrol* 15: 290-301, 2000.

12. **Feng X and Derynck R**. Specificity and versatility in TGF-b signaling through Smads. *Annu Rev Cell Dev Biol* 21: 659-693, 2005.
13. **Foley RN and Collins AJ**. End-stage renal disease in the Unites States: An update from the unites states renal data system. *J Am Soc Nephrol* 18: 2644-2648, 2007.
14. **Fujimoto M, Maezawa Y, Yokote K, Joh K, Kobayashi K, Kawamura H, Nishimura M, Roberts AB, Saito Y and Mori S**. Mice lacking Smad3 are protected against streptozotocin-induced diabetic glomerulopathy. *Biochem Biophys Res Commun* 305: 1002-1007, 2003.
15. **Gruszczynska-Biegala J, Pomorski P, Wisniewska MB and Kuznicki J**. Differential roles for STIM1 and STIM2 in store-operated calcium entry in rat neurons. *PLoS One* 6: e19285, 2011.
16. **Ha H and Lee HB**. Reactive oxygen species as glucose signaling molecules in mesangial cells cultured under high glucose. *Kidney Int Suppl* 58: S19-S25, 2000.
17. **Hayashida T and Schnaper HW**. Hihg ambient glucose enhances sensitivity to TGF-b1 via extracellular signal-regulated kinase and protein kinase Cd activities in human mesangial cells. *J Am Soc Nephrol* 15: 2032-2041, 2004.
18. **Heiling CW, Liu Y, England RL, Freytag SO, Gilbert JD, Heiling KO, Zhu M, Concepcion LA and Brosius FC**. D-glucose stimulates mesangial cell GLUT1 expression and basal and IGF-1-sensitive glucose uptake in rat mesangial cells: implication for diabetic nephropathy. *Diabetes* 46: 1030-1039, 1997.
19. **Hoffman BB, Sharma K, Zhu Y and Ziyadeh FN**. Transcriptional activation of transforming growth factor-b1 in mesangial cell culture by high glucose concentration. *Kidney Int* 54: 1107-1116, 1998.
20. **Hou M, Kuo H, Li J, Wang Y, Chang C, Chen W, Chiu C, Yang S and Chang W**. Orai1/CRACM1 overexpression suppresses cell proliferation via attenuation of the store-operated

calcium influx-mediated signaling pathway in A549 lung cancer cells. *Biochim Biophys Acta* 1810: 1278-1284, 2011.

21. **Isono M, Chen S, Hong SW, Iglesias-DE La Cruz MC and Ziyadeh FN**. Smad pathway is activated in the diabetic mouse kidney and Smad3 mediates TGF-beta-induced fibronectin in mesangial cells. *Biochem Biophy Res Commun* 296: 1356-1365, 2002.
22. **Kagami S, Border WA, Miller DE and Noble NA**. Angiotensin II stimulates extracellular matrix protein synthesis through induction of transforming growth factor-beta expression in rat glomerular mesangial cells. *J Clin Invest* 93: 2431-2437, 1994.
23. **Kaname S, Uchida S, Ogata E and Kurokawa K**. Autocrine secretion of transforming growth factor-b in cultured rat mesangial cells. *Kidney Int* 42: 1319-1327, 1992.
24. **Kanwar YS, Wada J, Sun L, Xie P, Wallner EI, Chen S, Chugh S and Danesh FR**. Diabetic nephropathy: mechanisms of renal disease progression. *Exp Biol Med* 233: 4-11, 2008.
25. **Lan HY**. Diverse roles of TGF-beta/Smads in renal fibrosis and inflammation. *Int J Biol Sci* 7: 1056-1067, 2011.
26. **Lan HY**. Transforming growth factor-b/Smad signalling in daibetic nephropathy. *Clin Exp Pharmacol Physiol* 39: 731-738, 2012.
27. **Leask A and Abraham DJ**. TGF-beta signaling and the fibrotic response. *FASEB J* 18: 816-827, 2004.
28. **Leung FP, yung LM, Yao X, Laher I and Huang Y**. Store-operated calcium entry in vascular smooth muscle. *Br J Pharmacol* 153: 846-857, 2007.
29. **Lewis RS**. The molecular choreography of a store-operated calcium channel. *Nature* 446: 284-287, 2007.

30. **Li J, Qu X, Ricardo SD, Bertram JF and Nikolic-Paterson DJ**. Reveratrol inhibits renal fibrosis in the obstructed kidney: potential rolel in deacetylation of Smad3. *Am J Pathol* 177: 1065-1071, 2010.

31. **Li JH, Huang XR, Zhu H, Johnson R and Lan HY**. Role of TGF-b signaling in extracellular matrix production under high glucose conditions. *Kidney Int* 63: 2010-2019, 2003.

32. **Lin X, Duan X, Liang Y, Su Y, Wrighton KH, Long J, Hu M, Davis CM, Wang J and Brunicardi FC**. PPM1A functions as a Smad phosphatase to terminate TGFb signaling. *Cell* 125: 915-928, 2006.

33. **Liu T and Feng XH**. Regulation of TGF-beta signaling by protein phosphatases. *Biochem J* 430: 191-198, 2010.

34. **Liu Y**. Renal fibrosis: new insights into the pathogenesis and therapeutics. *Kidney Int* 69: 213-217, 2006.

35. **Ma R, Smith S, Child A, Carmines PK and Sansom SC**. Store-operated Ca^{2+} channels in human glomerular mesangial cells. *Am J Physiol* 278: F954-F961, 2000.

36. **Mai, X., Shang, J., Liang, S., yu, B., Yuan, J., Lin, Y., Luo, R., Zhang, F., Liu, Y., Lv, X., Li, C., Liang, X., Wang, W., and Zhou, J.** Blockade of Orai1 store-operated calcium entry protects against renal fibrosis. J Am Soc Nephrol 27, 3063-3078. 2016.

37. **Mason RM and Wahab A**. Extracellular matrix metabolism in diabetic nephropathy. *J Am Soc Nephrol* 14: 1358-1373, 2003.

38. **Meng XM, Huang XR, Chung AC, Qin W, Shao X, Igarashi P, Ju W, Bottinger EP and Lan HY**. Smad2 protects against TGF-beta/Smad3-mediated renla fibrosis. *J Am Soc Nephrol* 21: 1477-1487, 2010.

39. **Mercer JC, Dehaven WI, Smyth JT, Wedel B, Boyles RR, Bird GS and Putney JW, Jr.** Large store-operated calcium-selective currents due to co-expression of orail1 or orail2 with the intracellular calcium sensor, STIM1. *J Biol Chem* 281: 24979-24990, 2006.

40. **Metwally SS, Mosaad YM, Nassr AA and Zaki OM**. Transforming growth factor-beta 1 in diabetic nephropathy. *Egypt J Immunol* 12: 103-112, 2005.

41. **Mima A, Matsubara T, Arai H, Abe H, Nagai K, Kanamori H, Sumi E, Takahashi T, Iehara N, Fukatsu A, Kita T and Doi T**. Angiotensin II-dependent Src and Smad1 signaling pathway is crucial for the development of diabetic nephropathy. *Lab Invest* 86: 927-939, 2006.

42. **Pan Z, Brotto M and Ma J**. Store-operated Ca^{2+} entry in muscle physiology and diseases. *BMB Rep* 47: 69-79, 2014.

43. **Parekh AB and Putney JW**. Store-operated calcium channels. *Physiol Rev* 85: 757-810, 2005.

44. **Poncelet A, De Caestecker MP and Schnaper HW**. The transforming growth factor-beta/Smad signaling pathway is present and functional in human mesangial cells. *Kidney Int* 56: 1354-1365, 1999.

45. **Pyram R, Kansara A, Banerji MA and Loney-Hutchinson L**. Chronic kidney disease and diabetes. *Maturitas* 71: 94-103, 2012.

46. **Runyan CE, Schnaper HW and Poncelet AC**. Smad3 and PKCd mediate TGF-b_1-induced collagen I expression in human mesangial cells. *Am J Physiol Renal Physiol* 285: F413-F422, 2003.

47. **Schena FP and Gesualdo L**. Pathogenetic mechanisms of diabetic nephropathy. *J Am Soc Nephrol* 16: S30-S33, 2005.

48. **Schnaper HW, Hayashida T, Hubchak SC and Poncelet AC**. TGF-beta transduction and mesangial cell fibrogenesis. *Am J Physiol Renal Physiol* 284: F243-F252, 2003.

49. **Shi Y and Massague J**. Mechanisms of TGF-b signaling from cell membrane to the nucleus. *Cell* 113: 685-700, 2003.

50. **Soboloff J, Spassova MA, Tang XD, Hewavitharana T, Xu W and Gill DL**. Orai1 and STIM reconstitute store-operated calcium channel function. *J Biol Chem* 281: 20661-20665, 2006.

51. **Steffes MW, Osterby R, Chavers B and Mauer SM**. Mesangial expansion as a central mechanism for loss of kidney function in daibetic patients. *Diabetes* 38: 1077-1081, 1989.

52. **Targos B, Baranska J and Pomorski P**. Store-operated calcium entry in physiology and pathology of mammalian cells. *Acta Biochim Pol* 52: 397-409, 2005.

53. **Throckmorton DC, Brogden AP, Min B, Rasmussen H and Kashgarian M**. PDGF amd TGF-b mediate collagen production by mesangial cells exposed to advanced glycosylation end products. *Kidney Int* 48: 111-117, 1995.

54. **Uehara A, Yasukochi M, Imanaga I, Nishi M and Takeshima H**. Store-operated Ca^{2+} entry uncoupled with ryanodine receptor and junctional membrane complex in heart muscle cells. *Cell Calcium* 31: 89-96, 2002.

55. **Wang A, Ziyadeh FN, Lee EY, Pyagay PE, Sung SH, Sheardown SA, Laping NJ and Chen S**. Interference with TGF-beta signaling by Smad3-knockout in mice limits diabetic glomerulosclerosis without affecting albuminuria. *Am J Physiol Renal Physiol* 293: F1657-F1665, 2007.

56. **Wang W, Koka V and Lan HY**. Transforming growth factor-b and Smad signalling in kidney diseases. *Nephrology* 10: 48-56, 2005.

57. **Wicks SJ, Lui S, Abdel-Wahab N, Mason RM and Chantry A**. Inactivation of Smad-transforming growth factor b signaling by Ca^{2+}-calmodulin-dependent protein kinase II. *Mol Cell Biol* 20: 8103-8111, 2000.

58. **Wolf G, Sharma K, Chen Y, Ericksen M and Ziyadeh FN**. High glucose-induced proliferation in mesangial cells is reversed by autocrine TGF-b. *Kidney Int* 42: 647-656, 1992.

59. **Wrighton KH and Feng X**. To (TGF) b or not to (TGF) b: Fine-tuning of Smad signaling via post-translational modifications. *Cell signal* 20: 1579-1591, 2008.

60. **Wu P, Ren Y, Ma Y, Wang Y, Jiang H, Chaudhari S, Davis ME, Zuckerman JE and Ma R**. Negative regulation of Smad1 pathway and collagen IV expression by store-operated Ca^{2+} entry in glomerular mesangial cells. *Am J Physiol Renal Physiol* 312: F1090-F1100, 2017.

61. **Wu P, Wang Y, Davis ME, Zuckerman JE, Chaudhari S, Begg M and Ma R**. Store-operated Ca^{2+} channel in mesangial cells inhibits matrix protein expression. *J Am Soc Nephrol* 26: 2691-2702, 2015.

62. **Xia L, Wang H, Munk S, Kwan J, Goldberg HJ, Fantus G and Whiteside CI**. High glucose activates PKC-z and NADPH oxidase through autocrine TGF-b_1 signaling in mesangial cells. *Am J Physiol Renal Physiol* 295: F1705-F1714, 2008.

63. **Xu L, Chen Y and Massague J**. The nuclear import function of Smad2 is masked by SARA and unmasked by TGFb-dependent phosphorylation. *Nat Cell Biol* 2: 559-562, 2000.

64. **Zuckerman JE and Davis ME**. Targeting therapeutics to the glomerulus with nanoparticles. *Adv Chronic Kidney Dis* 20: 500-507, 2013.

65. **Zuckerman JE, Gale A, Wu P, Ma R and Davis ME**. siRNA delivery to the glomerular mesangium using polycationic cyclodextrin nanoparticles containing siRNA. *Nucl Acid Ther* 25: 53-64, 2015.

FIGURE LEGENDS

Figure 1. Effect of SOCE on TGFβ1 secretion in cultured human MCs.

ELISA, showing TGFβ1 concentration in culture media. Confluent human MCs were incubated with serum free DMEM media for 72 h. One group was without any treatment (NT) and the other groups were treated with DMSO (1:1000) or TG (1 μM) for 8 h and 15 h prior to collection of media. DMSO and TG were present in the media throughout the period of treatment. 'n' indicates the number of independent experiments.

Figure 2. SOCE inhibited TGFβ1-induced phosphorylation of Smad3 in cultured human MCs.

A: Representative Western blot, showing changes in abundance of phosphorylated Smad3 (p-Smad3) and total Smad3 (Smad3) proteins in different treatment groups. Human MCs were treated with recombinant human TGFβ1 (5 ng/ml) in presence or absence of TG (1 μM) for 15 h. NT: the cells without any treatment, HCl: 4 mM HCl with 0.1% BSA at 1:4000, the vehicle control for TGFβ1. DMSO (1:1000): the vehicle control for TG. α-tubulin was used as the loading control. **B:** summary data, showing changes in the ratio of p-Smad3 to Smad3 in different treatment groups. ***$p<0.001$ vs NT and HCl; **$p<0.01$ vs TGFβ1 and TGFβ1 + DMSO. 'n' indicates the number of independent experiments.

Figure 3. Knockdown of Orai1 increased the TGFβ1-induced phosphorylation of Smad3.

A: Representative Western blot, showing effect of knockdown of Orai1 on phosphorylated Smad3 (p-Smad3) and total Smad3 (Smad3) protein abundance. Human MCs were without transfection (UT) or transfected with scramble (scr) or Orai1 siRNA (siOrai1). On day 3 after transfection cells were treated with TGFβ1 (5 ng/ml) in the presence or absence of TG (1 μM) for 15 h. α-tubulin was used as the loading control. L: protein ladder. **B:** Summary data from experiments presented in A. The abundance of p-Smad3 is expressed as the ratio of p-Smad3 to Smad3. **$p<0.01$ ***$p<0.001$ vs UT;

*p<0.05 vs TGFβ1, TGFβ1+Scr and TGFβ1+siOrai1+TG; #p<0.05 vs TGFβ1+siOrai1+TG; ##p<0.01 vs TGFβ1+siOrai1. 'n' indicates the number of independent experiments.

Figure 4. Overexpression of Orai1 decreased the TGFβ1-induced phosphorylation of Smad3.

A: Representative Western blot, showing phosphorylated Smad3 (p-Smad3) and total Smad3 (Smad3) protein abundance in human MCs in different groups. Human MCs were without transfection or were transfected with YFP plasmid (YFP) or mCherry-FLAG-Red Orai1 expression plasmid (Orai1). On day 2 after transfection, cells were treated with TGFβ1 (5 ng/ml) in the presence or absence of TG (1 μM) for 15 h. UT: cells without transfection and treatment, DMSO (1:1000): vehicle control for TG. α-tubulin was used as the loading control. **B:** Summary data showing changes in p-Smad3/ Smad3 ratio in different groups. ***p<0.01, vs UT; *p<0.05, vs TGFβ1, TGFβ1+DMSO, TGFβ1+Orai1+TG. 'n' indicates the number of independent experiments. **C:** Western blot, showing endogenous Orai1 and expressed Orai1 protein contents in human MCs transfected with YFP and Orai1. The expressed Orai1 protein was probed with primary antibody against Orai1 (the top panel) and flag (the middle panel). **D:** Effect of overexpression of Orai1 on SOCE in human MCs. Fura-2 fluorescence ratiometry was used to assess the intracellular Ca^{2+} concentration ($[Ca^{2+}]_i$) in MCs without transfection (untrans), transfected with YFP plasmid or mCherry-FLAG-Red Orai1 expression plasmid (Orai1). SOCE was evaluated using a Ca^{2+} re-addition protocol. TG (1 μM) was used to activate store-operated Ca^{2+} channels. ** denotes $P< 0.01$, compared to both Untrans and YFP groups. "n" indicates the number of cells analyzed in each group.

Figure 5. SOCE decreased TGFβ1-stimulated nuclear translocation of Smad3 in human MCs.

A: Representative Western blot, showing phosphorylated Smad3 (p-Smad3) protein abundance in nuclear extracts of human MCs. Human MCs were either without treatment (NT) or treated with recombinant human TGFβ1 (5 ng/ml) in the presence or absence of TG (1 μM) or a selective blocker of SOCE, La^{3+} (5 μM) for 15 h. HCl: vehicle control for TGFβ1, DMSO: vehicle control for TG. TBP was

used as the loading control for the nuclear proteins. L: protein ladder. **B:** Summary data from experiments presented in A. ***p<0.001, vs. NT and HCl; *p<0.05 vs. TGFβ1, TGFβ1+DMSO, TGFβ1+TG+La^{3+}. 'n' indicates the number of independent experiments. **C.** Representative images of immunofluorescence staining, showing Smad3 expression in human MCs treated with TGFβ1 (5 ng/ml) in the presence or absence of TG (1 μM) or GSK-7975A (10 μM) for 15 h. NT: cells without treatment, DMSO: vehicle control for TG. Smad3 is shown as red. Nuclei were stained with DAPI and shown as blue. Purple indicates co-localization of Smad3 with nuclei. Arrows indicate distribution of Smad3 in the cytosol. **D:** Summary data from 3 independent experiments, showing percentages of cells in which Smad3 was entirely localized in the nucleus in all cells counted. In each experiment, 3-4 fields were randomly selected and captured for analysis. ** denotes P<0.01, compared with NT group; †denotes P<0.01, compared with groups of TGFβ1, TGFβ1 + DMSO, and TGFβ1 + TG + GSK. The numbers under each bar (n) represent the total numbers of cells analyzed from 5 image fields per experiment of 3 independent experiments.

Figure 6. Distribution of NP-Cy3-siOrai1 in MCs in mouse kidney.

A: Representative images from 3 mice, showing localization of NP-Cy3-siOrai1 (red) in glomeruli (indicated by arrows), but not in tubules. Original magnification: 200X. **B:** Localization of NP-Cy3-siOrai1 in MCs (upper panel) but not in podocytes (lower panel), representative from 3 mice. MCs and podocytes were stained with Integrin-α8 (green) and synaptopodin (green), respectively. NP-Cy3-siOrai1 was shown as red signals. Original magnification: 200X.

Figure 7. Knockdown of Orai1 in MCs increased phosphorylation and nuclear translocation of Smad3 in mice.

A: Representative images for immuno-histochemical staining of phophosylated Smad3 (p-Smad3) on paraffin embedded kidney sections from NP-alone and NP-Cy3-siOrai1 injected mice. p-Smad3 staining is indicated as brown while nuclei are shown blue. Glomeruli are indicated by arrows. Original

magnification 200X. **B:** Magnified images of the region indicated by dashed boxes in A. **C:** Integrated density (ID) of phosphor-Smad3 staining averaged from 3 NP-Con mice and 3 NP-Cy3-siOrai1-treated mice. ** denotes P<0.01, compared to NP-Control. The numbers in parentheses under each bar represent the number of glomeruli counted from 5 sections per kidney. **D:** The percentage of cells without nuclear Smad3 in all cells counted in glomeruli, averaged from 3 NP-Con mice and 3 NP-Cy3-siOrai1-treated mice. ** denotes P<0.01, compared to NP-Control. The numbers in parentheses under each bar represent the number of glomeruli counted from 5 sections per kidney.

Figure 8. The diagram illustrating the negative regulation of TGFβ1-Smad3 signaling by SOCE in MCs.

p-Smad3: phosphorylated Smad3. Red line indicates inhibition and blue arrows indicate promotion of the pathway.

Figure 1

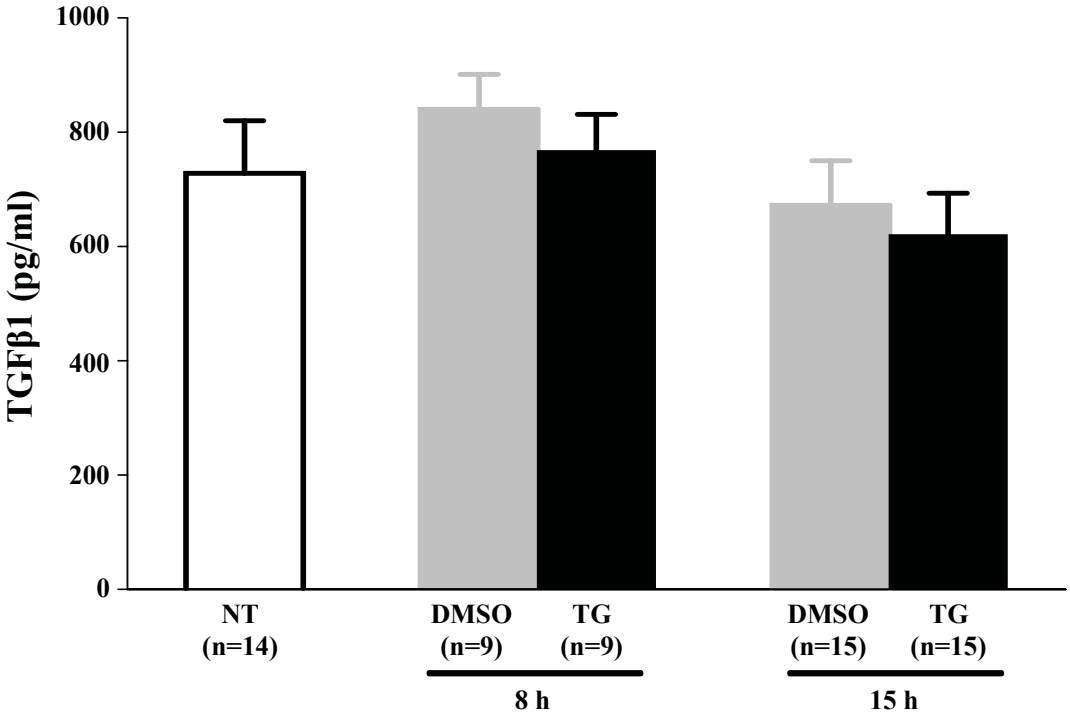
1000
800
600
400
200
0
TGFβ1 (pg/ml)
NT
(n=14)
DMSO
(n=9)
TG
(n=9)
8 h
DMSO
(n=15)
TG
(n=15)
15 h

Figure 2

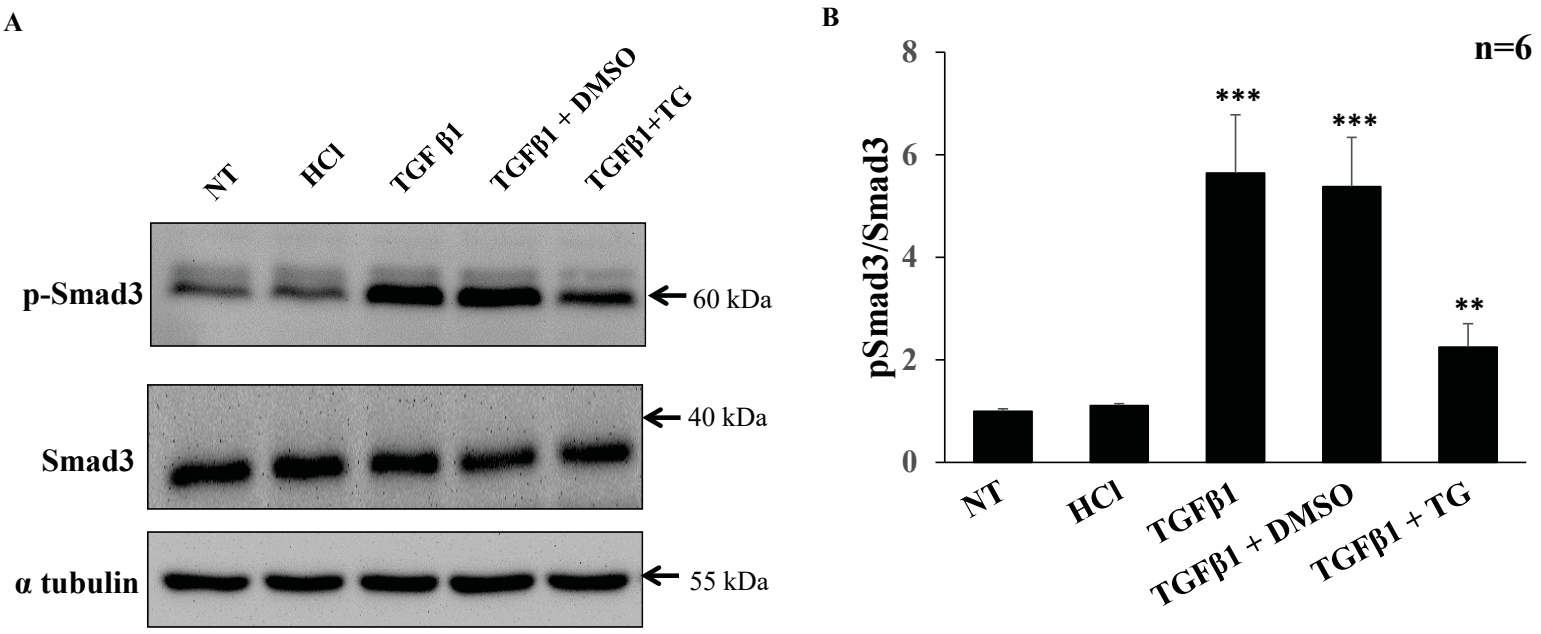
A
NT
HCl
TGF β1
TGFβ1 + DMSO
TGFβ1+TG
p-Smad3
60 kDa
Smad3
40 kDa
α tubulin
55 kDa
B
n=6
pSmad3/Smad3
0
2
4
6
8
***
***
**
NT
HCl
TGFβ1
TGFβ1 + DMSO
TGFβ1 + TG

Figure 3

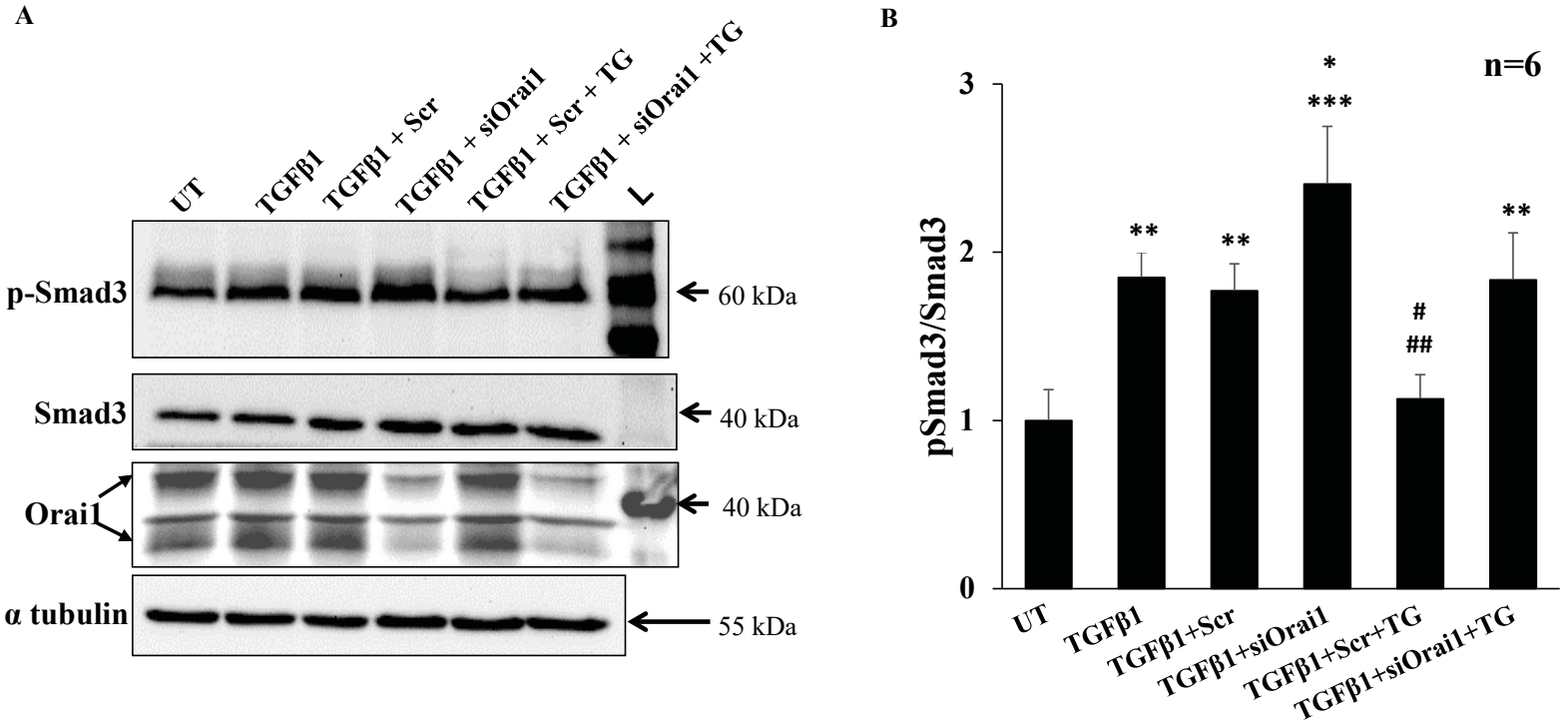
A
UT
TGFβ1
TGFβ1 + Scr
TGFβ1 + siOrai1
TGFβ1 + Scr + TG
TGFβ1 + siOrai1 +TG
L
p-Smad3
60 kDa
Smad3
40 kDa
Orai1
40 kDa
α tubulin
55 kDa
B
n=6
pSmad3/Smad3
0
1
2
3
*
***
**
**
**
#
##
UT
TGFβ1
TGFβ1+Scr
TGFβ1+siOrai1
TGFβ1+Scr+TG
TGFβ1+siOrai1+TG

Fig. 4

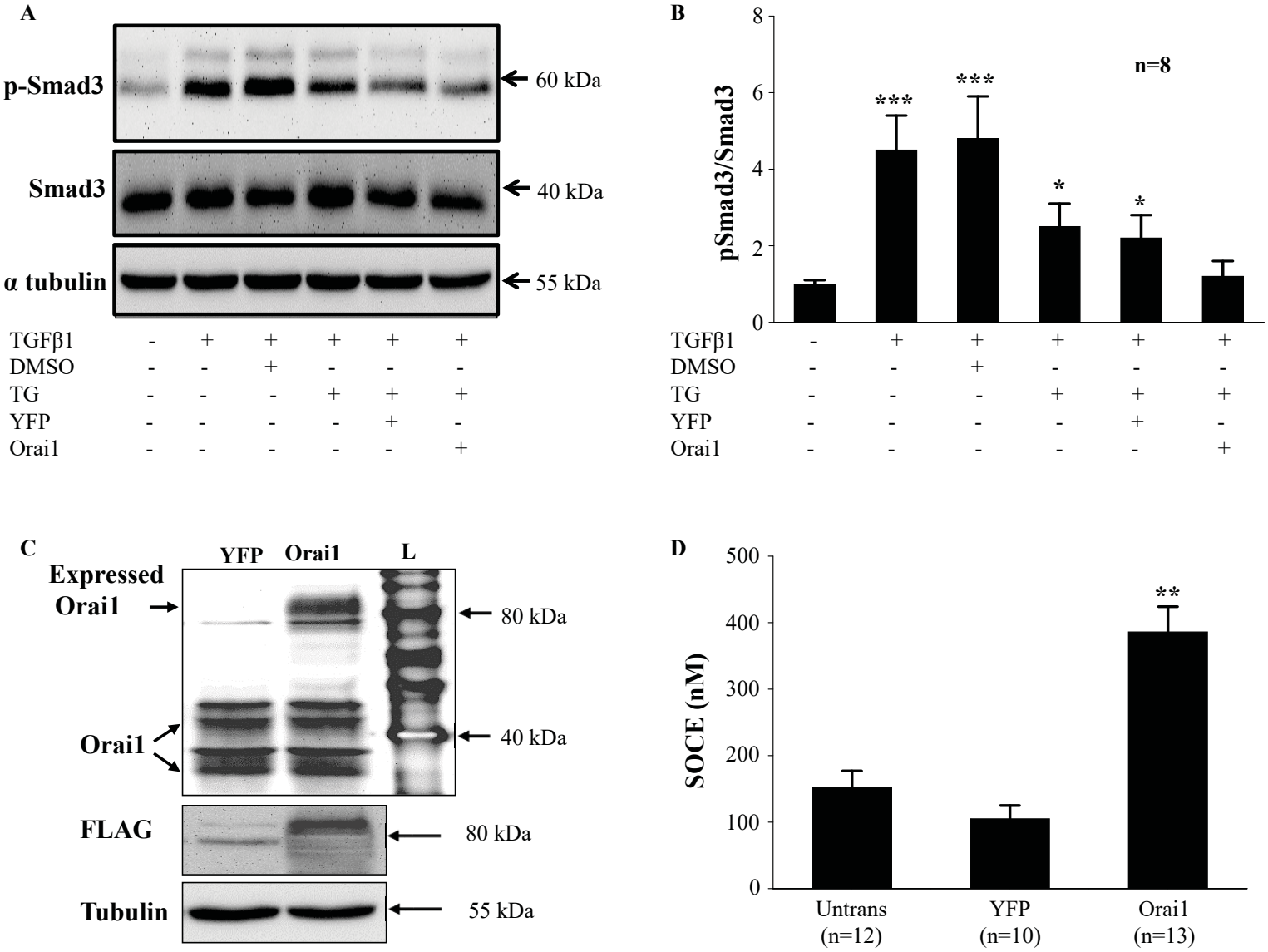
A
p-Smad3
Smad3
α tubulin
60 kDa
40 kDa
55 kDa
TGFβ1 - + + + + +
DMSO - - + - - -
TG - - - + + +
YFP - - - - + -
Orai1 - - - - - +
B
pSmad3/Smad3
n=8
***
***
*
*
TGFβ1 - + + + + +
DMSO - - + - - -
TG - - - + + +
YFP - - - - + -
Orai1 - - - - - +
C
YFP
Orai1
L
Expressed Orai1
Orai1
FLAG
Tubulin
80 kDa
40 kDa
80 kDa
55 kDa
D
SOCE (nM)
**
Untrans (n=12)
YFP (n=10)
Orai1 (n=13)

Fig. 5

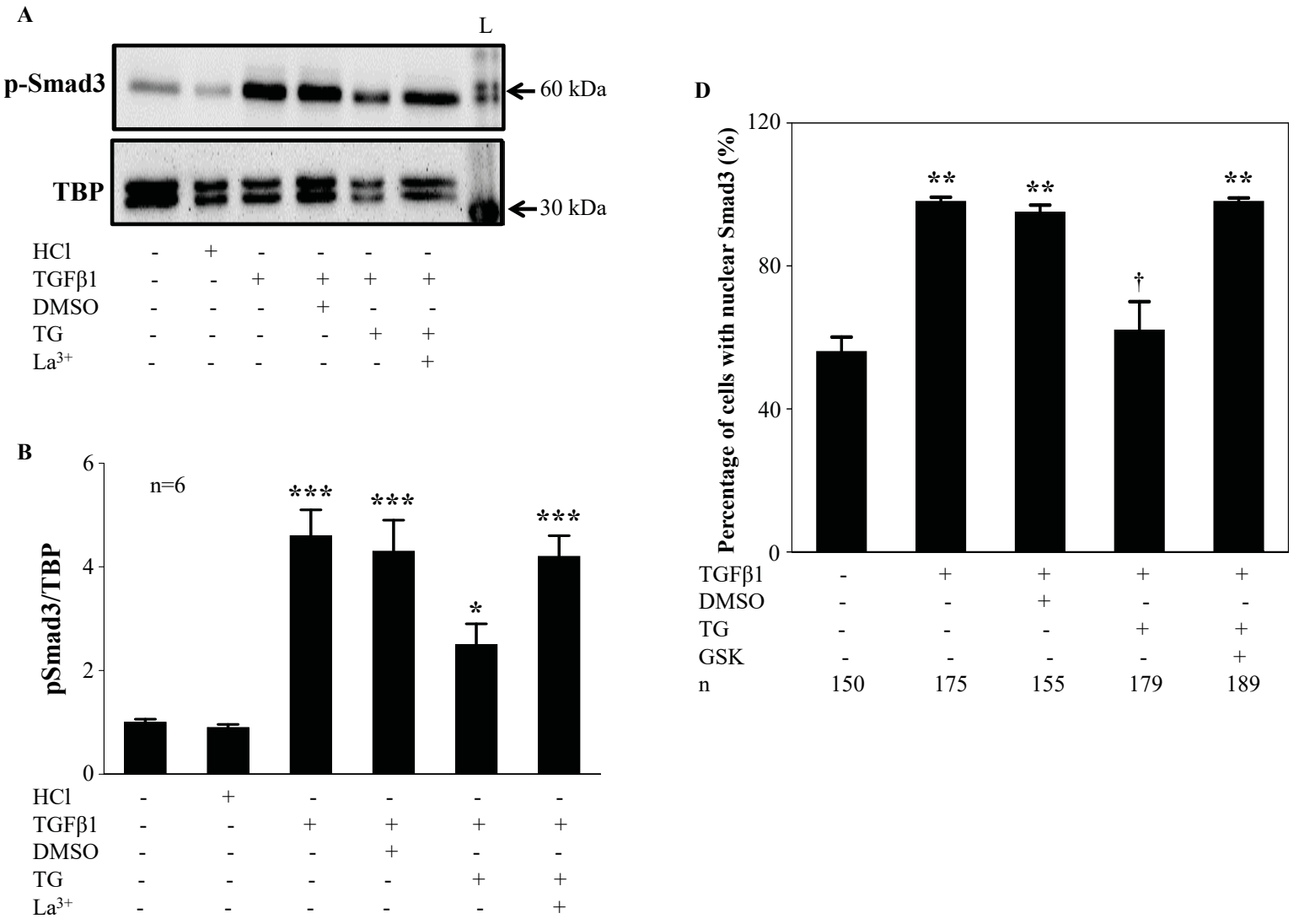
A
L
p-Smad3
60 kDa
TBP
30 kDa
HCl - + - - - -
TGFβ1 - - + + + +
DMSO - - - + - -
TG - - - - + +
La3+ - - - - - +
B
n=6
pSmad3/TBP
0
2
4
6
***
***
*
***
HCl - + - - - -
TGFβ1 - - + + + +
DMSO - - - + - -
TG - - - - + +
La3+ - - - - - +
D
Percentage of cells with nuclear Smad3 (%)
0
40
80
120
**
**
†
**
TGFβ1 - + + + +
DMSO - - + - -
TG - - - + +
GSK - - - - +
n 150 175 155 179 189

Figure 5

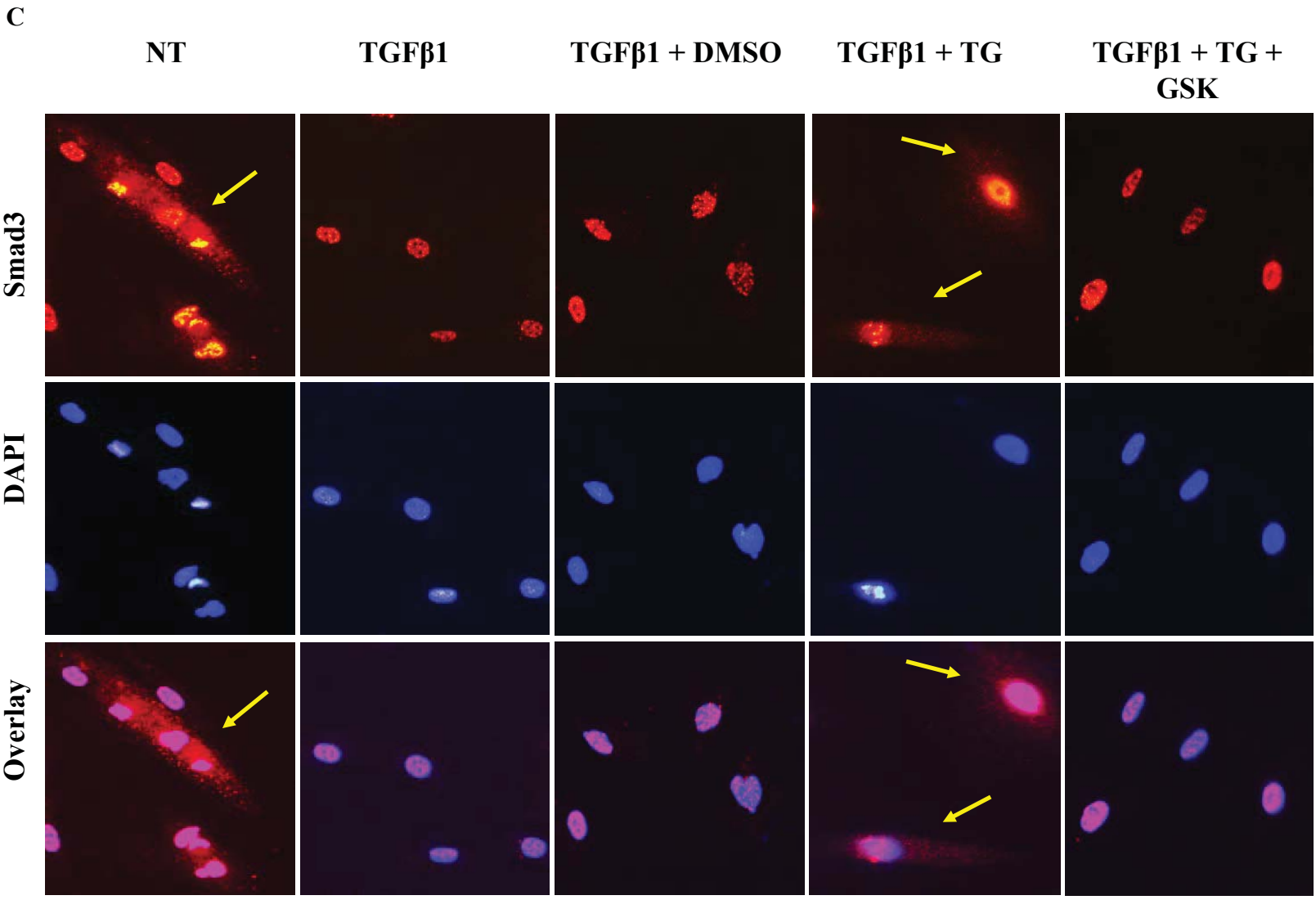
C
NT
TGFβ1
TGFβ1 + DMSO
TGFβ1 + TG
TGFβ1 + TG + GSK
Smad3
DAPI
Overlay

Figure 6

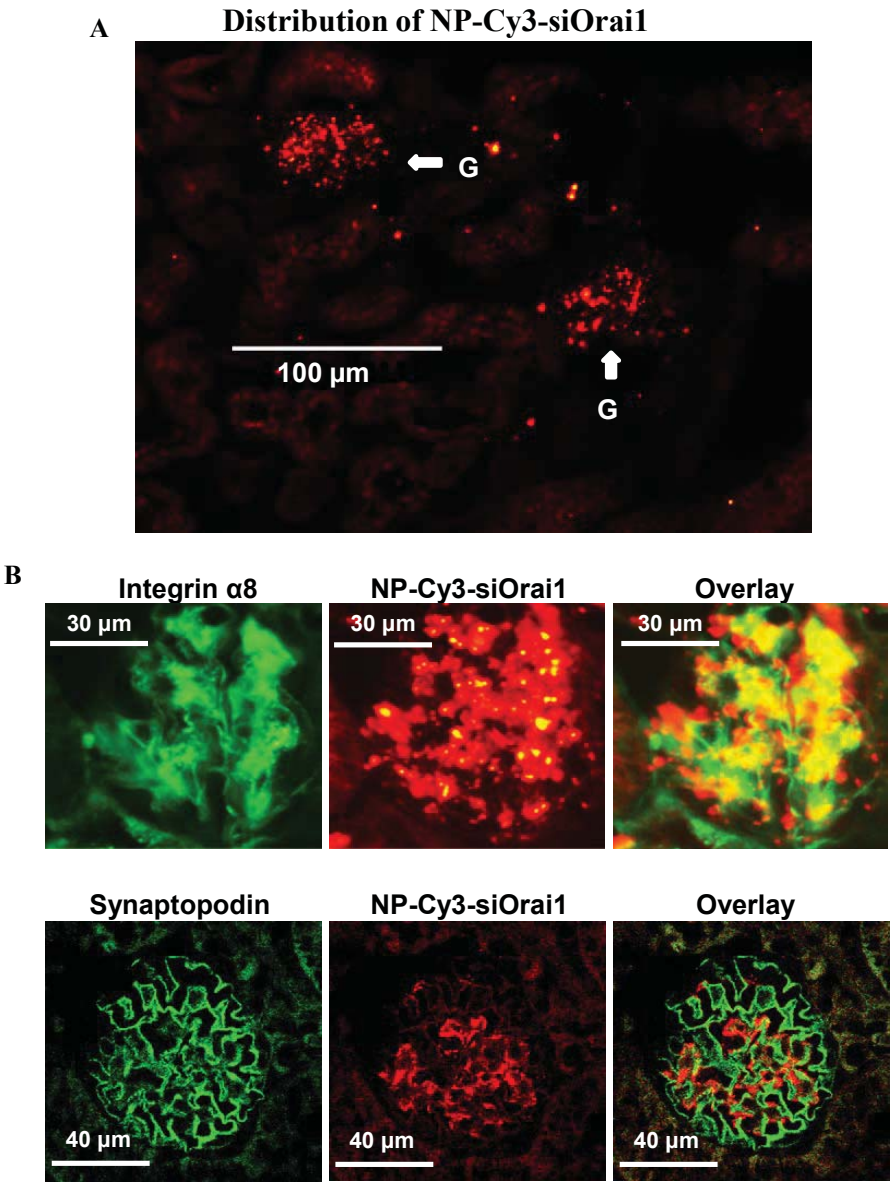
A
Distribution of NP-Cy3-siOrai1
G
100 μm
G
B
Integrin α8
NP-Cy3-siOrai1
Overlay
30 μm
30 μm
30 μm
Synaptopodin
NP-Cy3-siOrai1
Overlay
40 μm
40 μm
40 μm

Figure 7

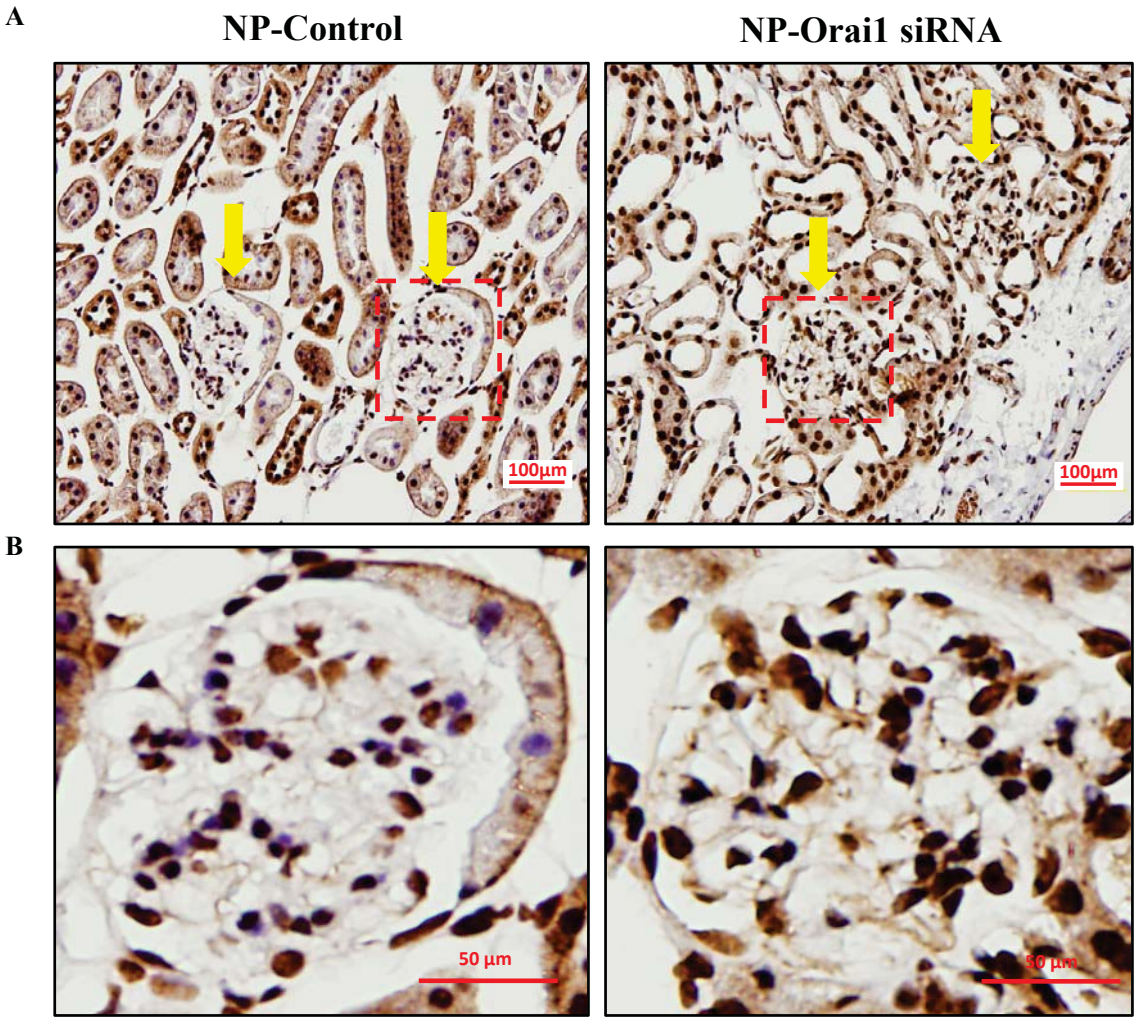

Fig. 7

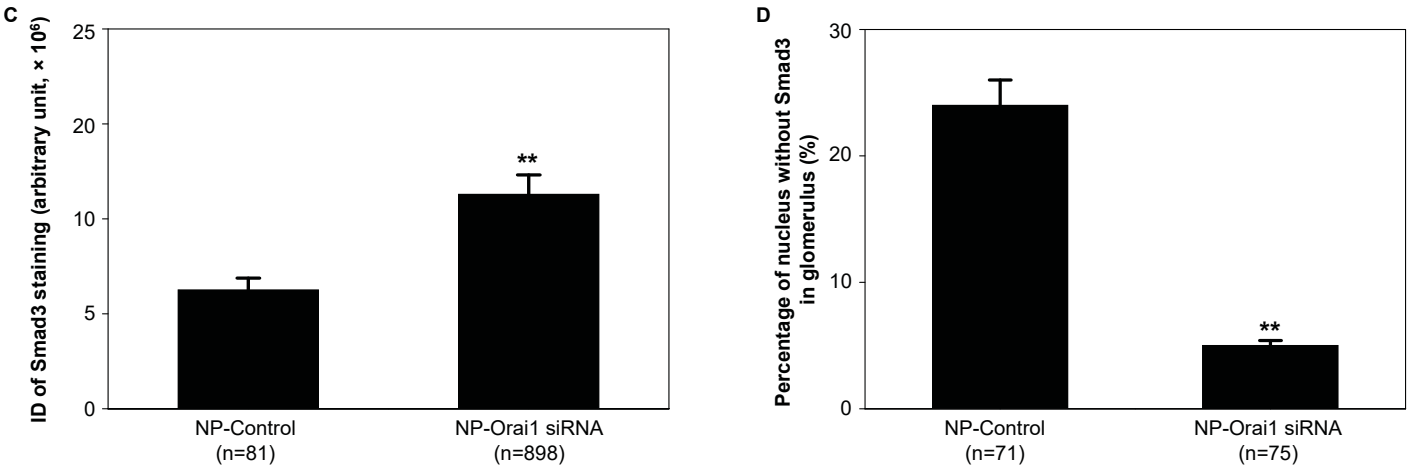
C
ID of Smad3 staining (arbitrary unit, × 10⁶)
25
20
10
5
0
**
NP-Control
(n=81)
NP-Orai1 siRNA
(n=898)
D
Percentage of nucleus without Smad3
in glomerulus (%)
30
20
10
0
**
NP-Control
(n=71)
NP-Orai1 siRNA
(n=75)

Figure 8

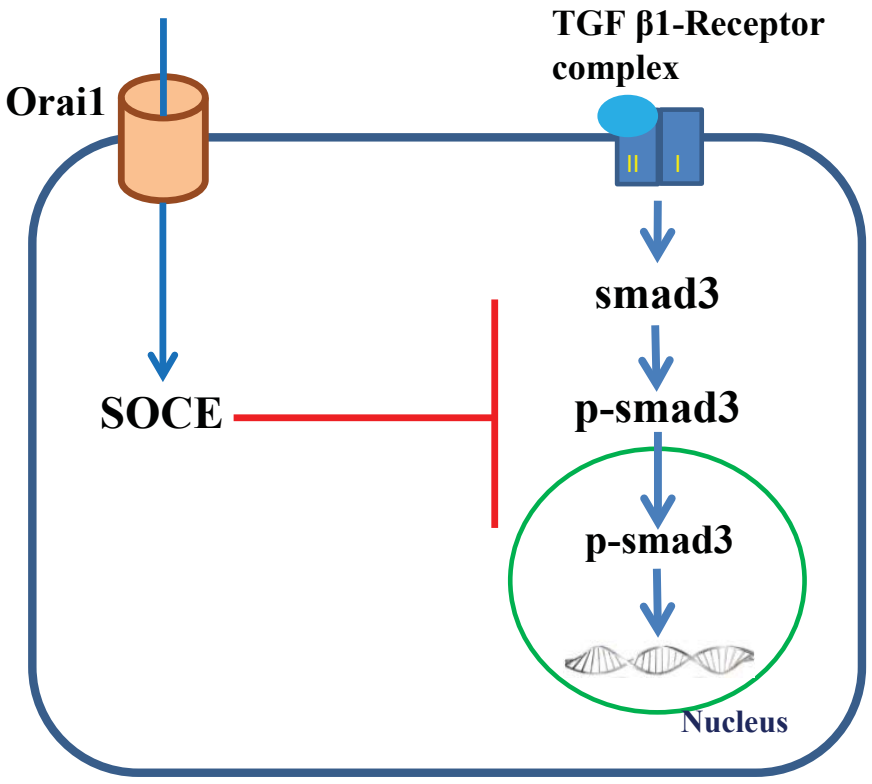
TGF β1-Receptor complex
Orai1
II
I
smad3
SOCE
p-smad3
p-smad3
Nucleus

Table1. siRNAs used for transient transfection.

siRNA	Sequence	Gene Accession number/ catalog number
ON_TARGETplus Non-targeting control siRNA#1 Target sequence	UGGUUUACAUGUCGACUAA	D-001810-01-20
Human Orai1 siRNA (sense strand)	5'-UGGAACUGUCGGUCAGUCUUAUGGC-3'	NM_032790
Cy3 Mouse Orai1 siRNA (sense strand)	5'-/5Cy3/ GGGUUGCUCAUCGUCUUUAGUGC-3'	NM_175423